Science and Technology, 2 (1997) 49-56

IGBT Based DC/DC Converter

M. Akherraz

Department of Electrical Engineering, College of Engineering, Sultan Qaboos University, P.O.Box 33, Al-Khod 123, Muscat, Sultanate of Oman.

تصميم وإنشاء محول كهربائي للتيار المستمر

محمد أخراز

خلاصة : هذا البحث هو عبارة عن دراسة نظرية وتحقيق تطبيقي معمقين على محول كهربائي لا مباشر من تيار مستمر إلى تيار مستمر اخر ذو خصوصيات متميزة . يتم هذا التحويل الكهربائي في مرحلتين . أولاً : يحول التيار المستمر إلى تيار متناوب عن طريق دائرة قطرية متكونة من أربعة ترانزستورات قوة من نوع الـ IGBT. ثانياً : يحول التيار المتناوب إلى تيار مستمر عبر حلقة وصل عالية التردد متبوعة بدائرة قطرية متكونة من ديودات سريعة . تحتوي حلقة الوصل على اربعة مكثفات مخمدة ومحول كهربائي ذو فجوة هوائية متغيرة . وقد تم تصميم هذه الحلقة العالية التردد بطريقة نظرية لتحقيق متطلب التحويل اثناء جهد معادل للصفر . وقد تمت محاكاة سيرة المحول الكهربائي المقترح في هذا المشروع عن طريق البرنامج الحاسوبي Pspice. كما تم تصميم وإنشاء وفحص نموذج اولي لهذا المحول في المختبر . ولاستكمال هذه الدراسة العلمية والهندسية ، تمت المقارنة الشاملة بين نتائج محاكاة سيرة المحول المدروس عبر Pspice ، والنتائج التي تم الحصول عليها تطبيقيا ، مع التعليق على التطابق بين هذه النتائج .

ABSTRACT: This paper presents an in-depth analytical and experimental investigation of an indirect DC-DC converter. The DC-AC conversion is a full bridge based on IGBT power modules, and the AC-DC conversion is done via a high frequency AC link and a fast diode bridge. The AC link, which consists of snubbing capacitors and a variable air-gap transformer, is analytically designed to fulfill Zero Voltage Commutation requirement. The proposed converter is simulated using PSPICE and a prototype is designed, built and tested in the laboratory. PSPICE simulation and experimental results are presented and compared.

Indirect DC-DC converters are increasingly becoming a viable option as Switched Mode Power Supplies (SMPS) for a variety of industrial applications (Bhat, 1991; Lo *et al*, 1992; Jan, 1992). Their important advantages of low losses, reduced EMI and low noise, make them very suitable for high frequency, low to medium power dc-dc conversion as well as low to medium power supplies of electric drives (Steigerwald, 1984; Kazimierczuk *et al*, 1992).

It is known that classical power supplies offer the advantages of simplicity, sturdiness and high reliability. However, for obvious reasons, they present major drawbacks whenever the size and weight of a power supply is critical. In the last decade, SMPS have offered clean solutions to these drawbacks. However, a further reduction of weight and size of SMPS calls for higher operating frequency. This means that the power switches are severely stressed and commutation losses are tremendously increased. Recently, it is believed that the exploitation of LC resonance at commutation is offering an adequate solution to the above mentioned limitations of SMPS (Severns, 1992; Bose, 1992). These new generations of DC-DC converters have gained a widespread interest and use in specialized laboratories, universities and industrial applications, (Bhat, 1993; Ninomiya *et al*, 1991; Morrison, 1992; Bose, 1992 and Akherraz, 1993).

This paper presents an in-depth analytical and experimental investigation of an indirect dc-dc converter. The technical characteristics of the proposed converter are: i) DC input voltage 300V ii) Adjustable dc output voltage (via the switching duty cycle), iii) Switching frequency 24KHz, and iv) Commutation time less than 5% of the operating period.

The main features of this converter are fourfold: i) Low switching losses due to commutation at resonance ii) Clean AC link voltage and current waveforms due to the design of an air-gaped transformer in the ac link, iii) High efficiency, and iv) Fast IGBT power modules as main switches.

This paper is organized in three parts. In the first part, the state variables of the switching commutation intervals are defined and solved in closed form fashion. The second part outlines the PSPICE simulation results of the investigated converter. The third part presents the experimental results with discussion and comments on the performances obtained.

Switching commutation intervals

The proposed converter is shown in figure 1. T_1, T_2, T_1' and T_2' are IGBT power modules with anti-parallel diodes. C_1, C_2, C_1' and C_2' are snubbing capacitors. L_f is transformer primary leakadge inductance, L_s and C_s are the output filter components and R is the load. The AC link transformer is a mid-point type with a variable air-gap and a unity turn-ratio.

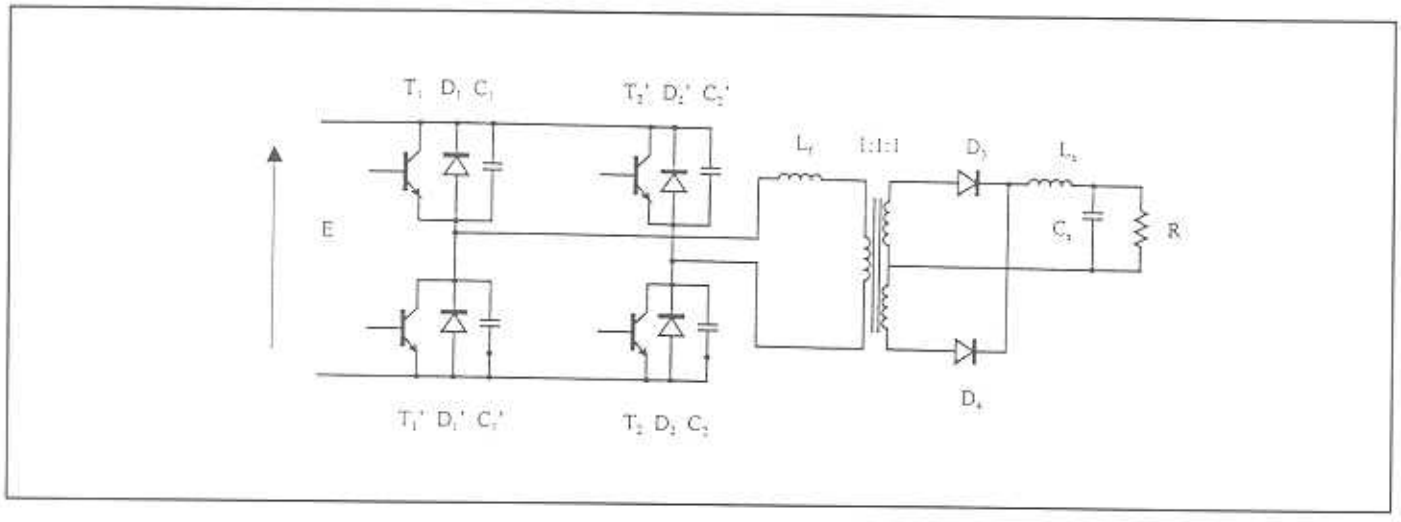

Figure 1. PSPICE simulation results of DC/DC resonant commutation converter.

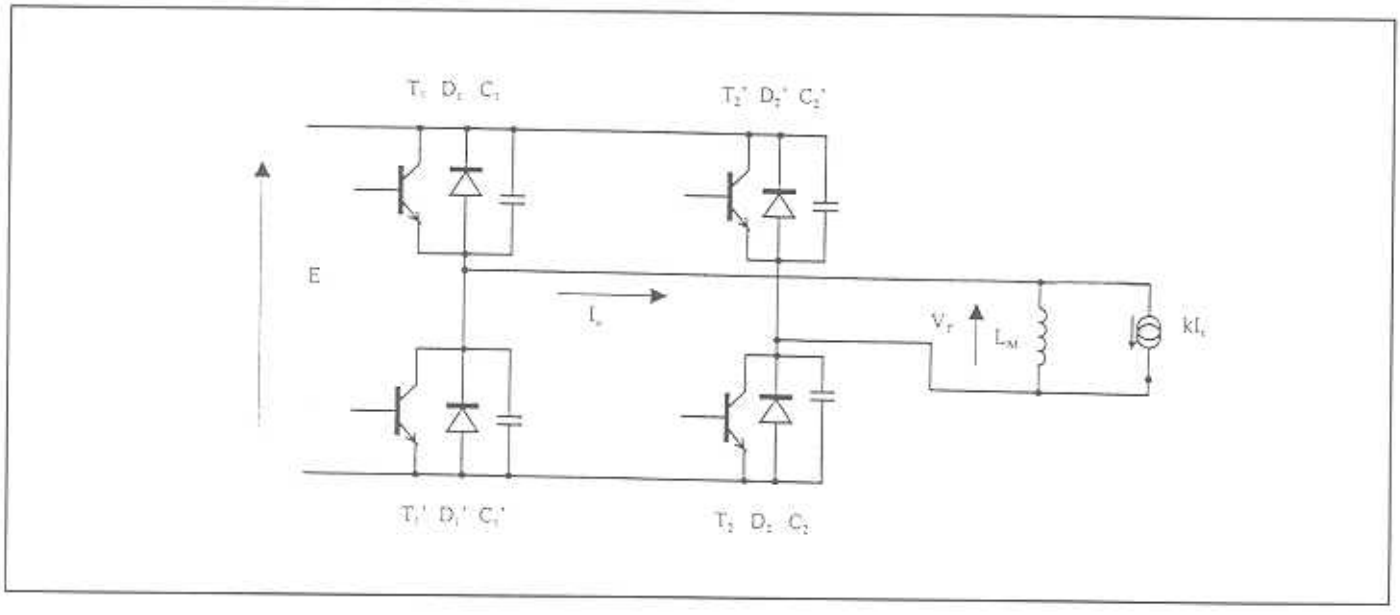

Figure 2. Summary of salient experimental results of the proposed DC/DC conversion.

The analysis of the commutation intervals is carried out under the following assumptions: i) IGBTs and diodes are ideal switches ii) The snubbing capacitors C_1, C_2, C_1' and C_2' are identical. Their capacitance is equal to C_o. iii). All circuit resistances are neglected, and iv) Negligible primary and secondary leakage inductances.

The obtained simplified converter's equivalent circuit, referred to the transformers primary is shown in figure 2. L_m is the magnetizing inductance. kI_s symbolizes the bridge and the load ($k = \pm 1$).

The initial commutation interval is assumed to be (T_1, T_2 On) and k=1. Then, starting at the time when T_1 and T_2 are turned off and until T_1' and T_2' are turned on and k= -1, the commutation goes through two operating intervals.

INTERVAL A: T_1, T_2 are off and k=1. The equivalent circuit of the investigated converter, during this interval, is shown in figure 3. The corresponding voltage and current equations are as follows:

$$V_T = L_m \, dI_m/dt \quad (1)$$

$$I_u = I_m + I_s \quad (2)$$

$$I_{c1} + I_{c1} > = 0 \quad (3)$$

$$2V_{c1} + V_T = E \quad , \quad (4)$$

where V_T is the transformer primary voltage, I_u is the AC link current (or transformer primary current) and I_m is the transformer magnetizing current. Since the commutation energy is provided by the LC resonance, the input line current is equal to zero during commutation. Combining equations (1) to (4), the following second order differential equation is obtained:

$$d^2I_m/dt^2 + \omega_o^2 \, I_m = - \omega_o^2 \, I_s \quad , \quad (5)$$

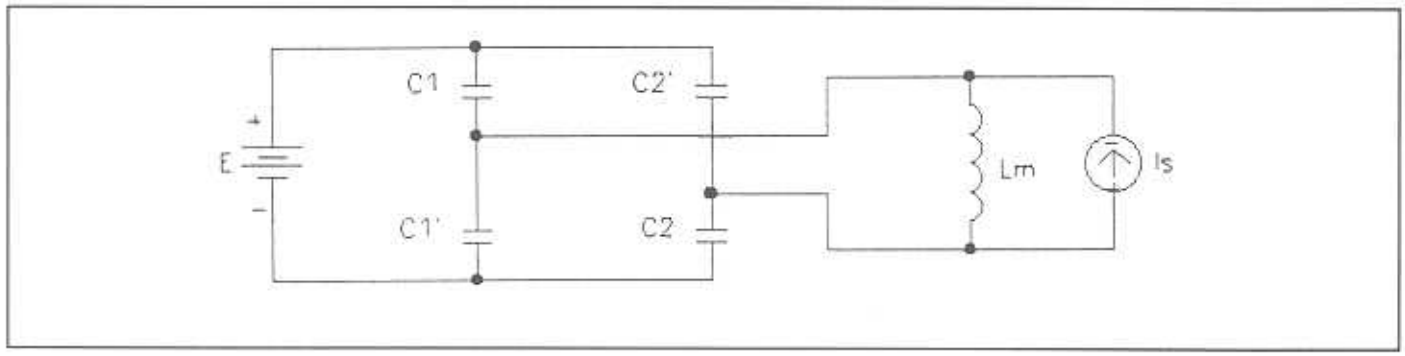

Figure 3. Equivalent circuit of the converter during commutation interval A.

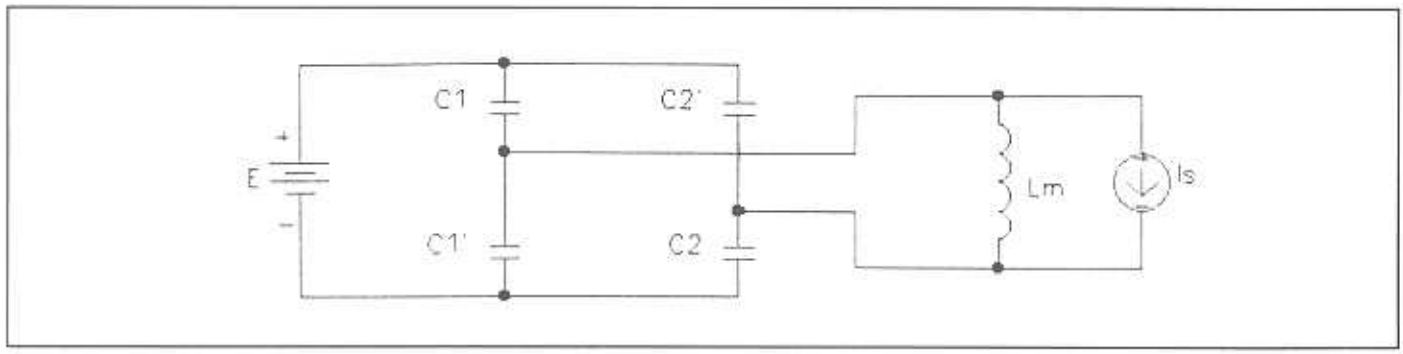

Figure 4. Equivalent circuit of the converter during commutation interval B.

where $\omega_o^2 = 1/(L_m C_o)$. The initial conditions of equation (5) are $V_{c1} = V_{c2} = 0$; $V'_{c1} = V'_{c2} = E$ and $I_m = I_{mo}$. The initial magnetizing current I_{mo} is determined later in this paragraph. With these initial conditions, solving for equation (5) leads to the following:

$$I_m = E/(L_m\omega_o) \sin(\omega_o t) + (I_{mo} + I_s) \cos(\omega_o t) - I_s \quad (6)$$

$$V_T = E \cos(\omega_o t) - L_m\omega_o (I_{mo} + I_s) \sin(\omega_o t) \quad (7)$$

$$I_u = E/(L_m\omega_o) \sin(\omega_o t) + (I_{mo} + I_s) \cos(\omega_o t) \quad (8)$$

$$V_{c1} = E(1 - \cos(\omega_o t)) + L_m\omega_o (I_{mo} + I_s) \sin(\omega_o t) \quad (9)$$

This interval ends when V_T crosses zero, i.e. I_m is at maximum. This occurs at $t=t_{41}$ given by:

$$\text{Tan}(\omega_o t_{41}) = E/((L_m\omega_o)(I_{mo} + I_s)) \quad (10)$$

At $t= t_{41}$, all capacitor voltages are equal to E/2, the transformer voltage is null and the AC link current is surpassing I_s.

INTERVAL B: T_1, T_2 are off and k=-1. The converters equivalent circuit, during this interval, is shown in figure 4. Similarly to interval A, the magnetizing current I_m is given by the following differential equation:

$$d^2I_m/dt^2 + \omega_o^2 I_m = \omega_o^2 I_s \quad (11)$$

The initial conditions are obtained by setting $t= t_{41}$ in equations (6) to (9). The obtained solutions are as follows:

$$I_m = (I_m(t_{41}) - I_s) \cos(\omega_o t) + I_s \quad (12)$$

$$V_T = -L_m\omega_o (I_m(t_{41}) - I_s) \sin(\omega_o t) \quad (13)$$

$$I_u = (I_m(t_{41}) - I_s) \cos(\omega_o t) \quad (14)$$

$$V_{c1} = E/2 + L_m\omega_o/2 (I_m(t_{41}) - I_s) \sin(\omega_o t) \quad (15)$$

In order to achieve the appropriate operation, i.e. commutation at zero voltage, C_1 ought to be charged to E prior to I_u reaching zero. This condition can be obtained from equation (15) by setting the magnitude of the sinusoidal term to a value greater than E/2, i.e.

$$L_m\omega_o (I_m(t_{41}) - I_s) = \lambda E \quad (16)$$

where λ is a coefficient greater than unity. Using this coefficient as a parameter, the initial magnetizing current I_{mo} is given by the following equation:

$$I_{mo} = \text{SQRT}\{(\lambda E + 2I_s L_m\omega_o)^2 - E^2\}/(L_m\omega_o) - I_s \quad (17)$$

The maximum magnetizing current takes place at the end of interval A, i.e. at $t= t_{41}$, and is given by:

$$I_{m,max} = \lambda E/(L_m\omega_o) + I_s \quad (18)$$

The second interval ends when C_1 is charged to E. This occurs at $t = t_{42}$ given by:

$$\sin(\omega_o t_{42}) = 1/\lambda \quad (19)$$

At $t = t_{42}$, C_1' is completely discharged. T_1' and T_2' can be smoothly triggered. Thus, with T_1' and T_2' conducting and k=-1, the commutation is over. It appears that L_m and C_o play a crucial role in providing adequate commutation. Therefore, they are particularly dimensioned to satisfy the following conditions: i) Appropriate commutation, i.e. $\lambda >= 1$; ii) Commutation time (i.e. $t_{41} + t_{42}$) <= 5% switching period; and iii) Imposed maximum magnetizing current during commutation. The design of L_m and C_o is presented in the next paragraph.

PSPICE Simulation

PSPICE MODELING: The investigated converter is simulated using PSPICE. Each IGBT power module is represented by an n-channel enhancement type MOSFET supplying base current, through a variable resistance R_{mod}, to a PNP-NPN transistors connected in a gate-less thyristor type circuit, as shown in figure 5. The n-channel MOSFET is modeled as an intrinsic MOSFET with series resistances with the drain and source, and shunt resistance with the drain source channel. The PNP-NPN transistors are represented by the enhanced Gummel-Pool models (Rashid, 1993). The air-gap transformer is represented by a variable magnetizing inductance and an ideal transformer. The diodes are modeled with the appropriate parasitic resistance and capacitance (R_s and C_{jo}) (Rashid, 1993).

DESIGN OF L_m AND C_o : The investigated converter is PSPICE simulated for the following operating point conditions:
E = 300V , I_s = 0.5 A, $I_{m,max}$ = 1.5 A; switching frequency f = 24kHz, switching period T = 41.6 µsec, and commutation time = 5% T. The key equations used for designing L_m and C_o are derived from the equations given in the previous paragraph, in the following fashion. Given a value of λ (> 1), ω_o, I_{mo}, t_{41}, t_{42}, L_m and C_o are calculated, respectively, as follows:

$$(\sqrt{(\lambda^2 - 1)} + \sqrt{(4\lambda^2 - 1)})/(2\lambda^2) = \sin(0.05\, T\, \omega_o) \quad (20)$$

$$I_{mo} = \sqrt{(4\lambda^2 - 1)}/\lambda - I_s \quad (21)$$

$$\sin(\omega_o t_1) = 2\lambda / (1 + \lambda^2 (I_{mo} + I_s)^2) \quad (22)$$

$$\cos(\omega_o t_2) = 2 (I_{mo} + I_s) \lambda^2 / (1 + \lambda^2 (I_{mo} + I_s)^2) \quad (23)$$

$$L_m = \lambda E / \omega_o \quad (24)$$

$$C_o = 1 / L_m \omega_o^2 \quad (25)$$

PSPICE SIMULATION RESULTS: The investigated converter is simulated using PSPICE for the following operating point conditions:
E = 300V , I_s = 0.5 A , $I_{m,max}$ = 1.5 A ; switching frequency f = 24kHz, switching period T = 41.6 µsec. Commutation time = 5% of the period T. Variety of values of λ are employed in order to simulate the behavior of the investigated converter during commutation. The obtained waveforms are in good agreement with the analytical predictions, especially for values of λ = 1.225. To illustrate this concordance as well as the conformity of the proposed PSPICE model, the cases of λ = 1.5 and λ = 1.225 are presented in this paragraph. Figures 6 and 7 show the capacitor voltage V_{c1}, the capacitor current I_{c1}, the transformer primary current I_T and the transformer magnetizing current I_M for λ=1.5 and λ=1.225, respectively. The main comments about these waveforms are threefold: i) The peak-to-peak primary current and magnetizing current are 4.4A and 3.4A, respectively, and 4.6A and 3.6A, respectively, for λ=1.5 and λ=1.225, ii) I_{c1} current spikes are less than 1A (i.e. 20 to 25 % the ppk AC currents), and iii) Commutation time is within the range of 2 µsec. The obtained quantitative results are summarized in table 1.

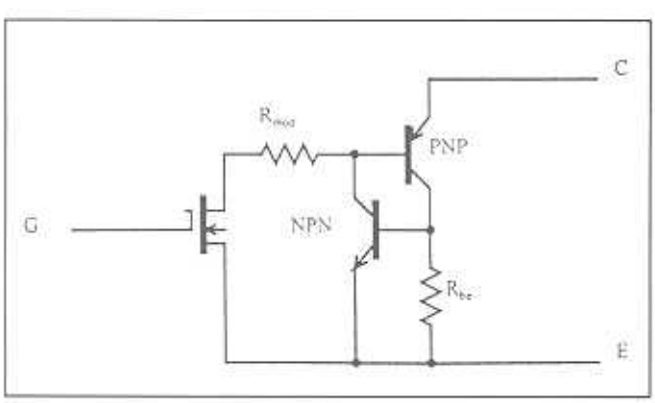

Figure 5. Equivalent circuit of a power IGBT module.

TABLE 1

PSPICE Simulation results of DC/DC resonant commutation converter.

λ	L_m (mH)	C_o (nF)	I_{mo} (A)	t_{41} (µsec)	t_{42} (µsec)
1.0	0.3	3.32	1.232	0.522	1.566
1.118	0.446	3.96	1.289	0.616	1.471
1.225	0.556	4.12	1.326	0.638	1.449
1.5	0.876	4.33	1.386	0.662	1.421

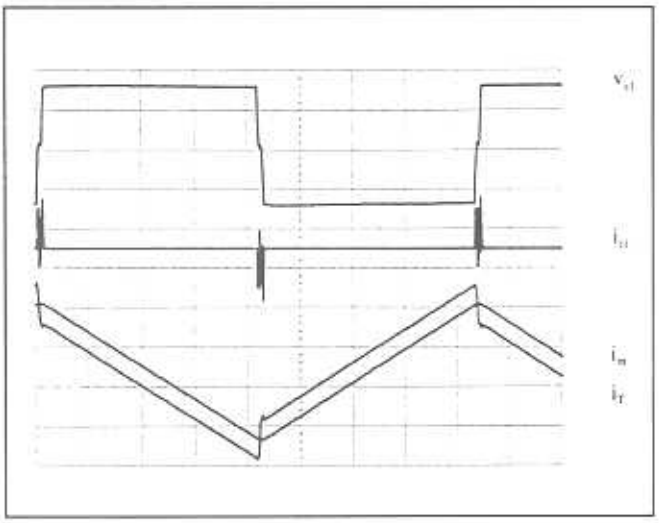

Figure 6. PSPICE generated current and voltage wave-forms in case of λ=1.5.

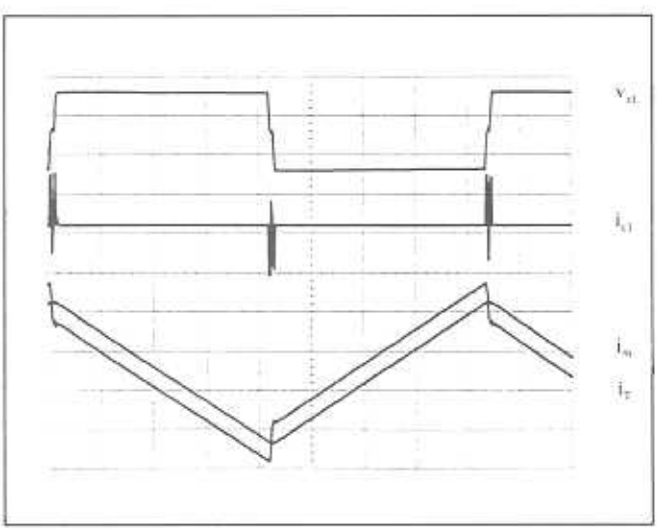

Figure 7. PSPICE generated current and voltage wave-forms in case of λ=1.225.

Experimental results - Presentation and discussion

The proposed converter is designed, built and tested in the laboratory. The input voltage and switching frequency are set to 300V and 24 kHz, respectively. The characteristics of the IGBT power modules are as follows: V_{ces} = 1200V, I_c = 25A, V_{cesat} = 3V, t_{on} = 400ns, t_s = 500ns and t_f = 200ns. The IGBT's triggering circuit synoptic diagram is described in figure 8.The performances of the investigated converter are tested under variable loading conditions and variable air-gap. Salient results are presented in this paragraph. Figures 9 and 10 show the capacitor voltage V_{c1}, its corresponding current I_{c1} and the T_1 transistor current I_{t1}. They are obtained with an air gap of 0.3 mm. From figure 9, it can be seen that C_1 is indeed discharged, prior to the switching of T_1'. I_{c1} spikes are drastically reduced and the commutation is improved. Figure 10 shows the commutation in more details.

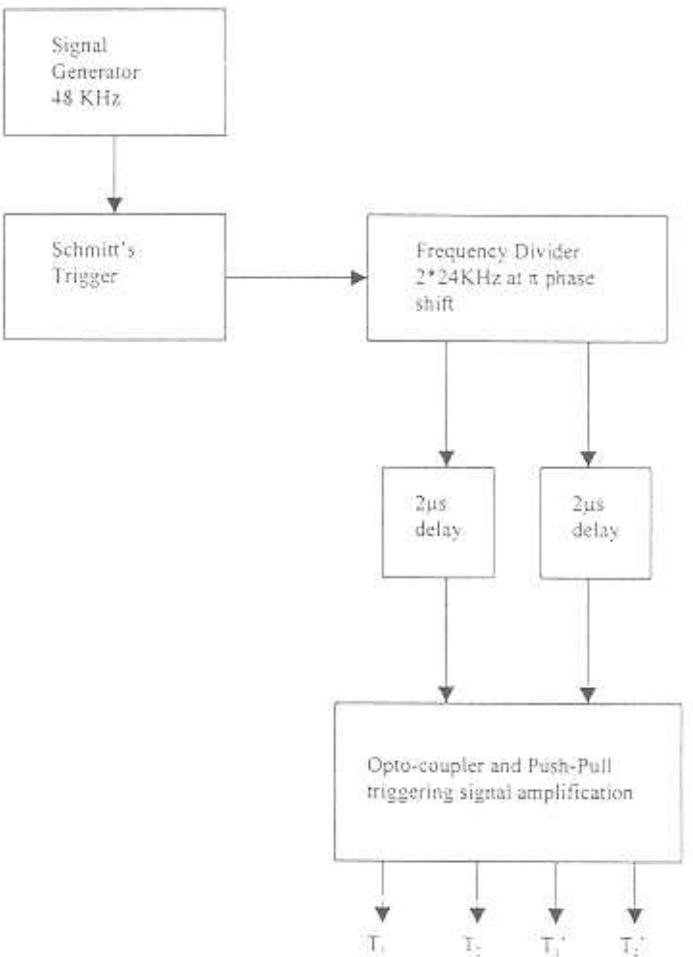

Figure 8. Synoptic diagram of the IGBT's triggering circuit.

The obtained commutation time is about 2µsec, which represents 4.8% of the operating period. A further increase of the air-gap to 1.5 mm has lead to the results shown in figures 11 and 12. The commutation time is increased to 2.3 µs (5.6% of the period) and slight commutation spikes re-appear at the capacitor current I_{c1}.

The obtained waveforms are as predicted theoretically, through the state variable equations derived in the second paragraph of this paper, and by PSPICE simulation. Prior to reaching E, V_{c1} crosses E/2 at t_{41}, and changes slope to get to E at t_{42}. Also, the AC-link current drops from a maximum value at t_{41}, and oscillates in a damped fashion until t_{42}, after which it continues to decrease (or increase) linearly until the next commutation.

A minor difference is observed between PSPICE and experimental results. For instance, for a switching frequency of 24kHz and a load of 1.2Kw, PSPICE predicts a commutation time of 2.06µsec with a theoretical magnetizing inductance of 0.3 mH. The corresponding experimental commutation time is about 2.3µsec with an air-gap of 1.5mm and a measured magnetizing inductance of 0.47mH.

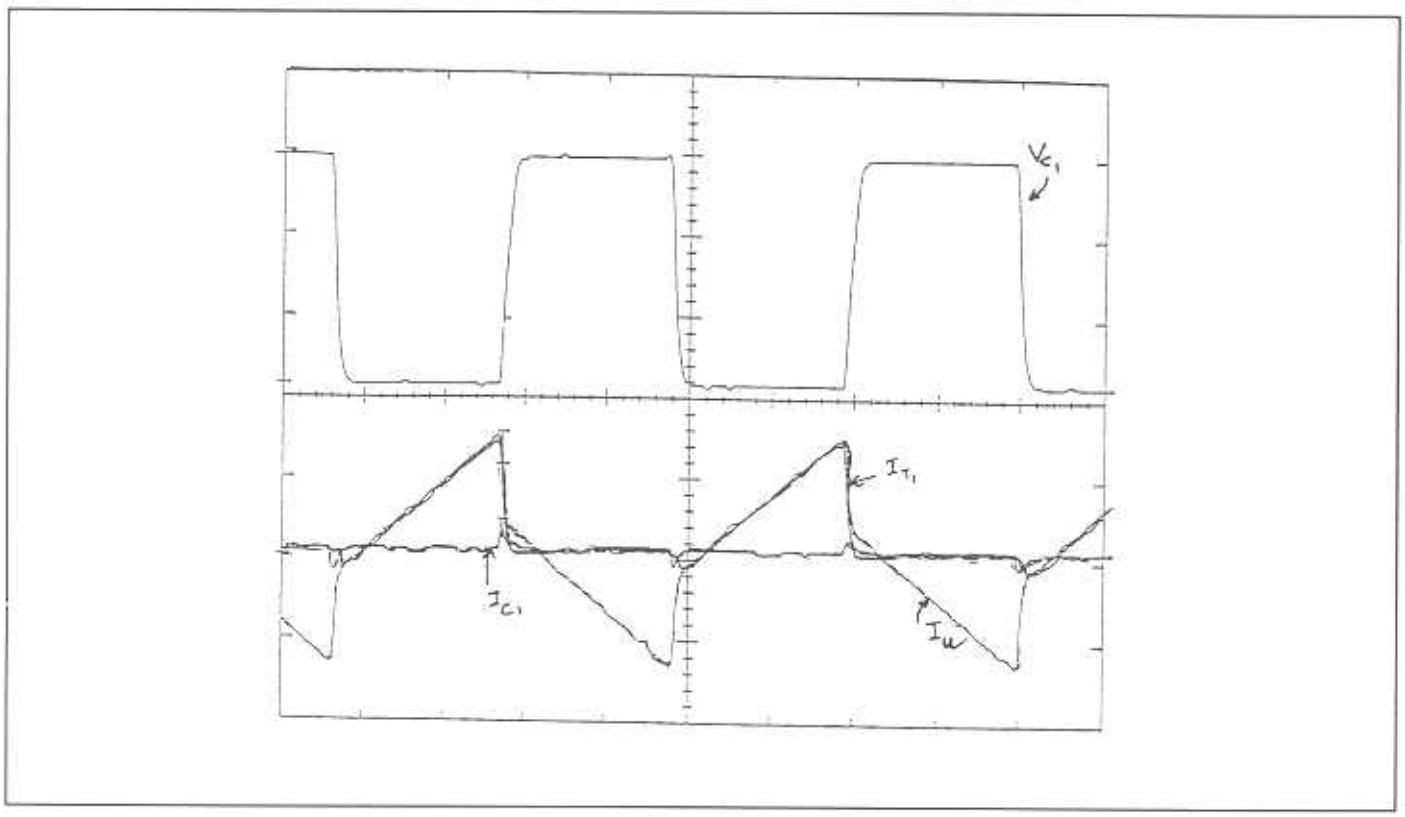

Figure 9. Voltage and current waveforms obtained with an air gap of 0.3 mm.

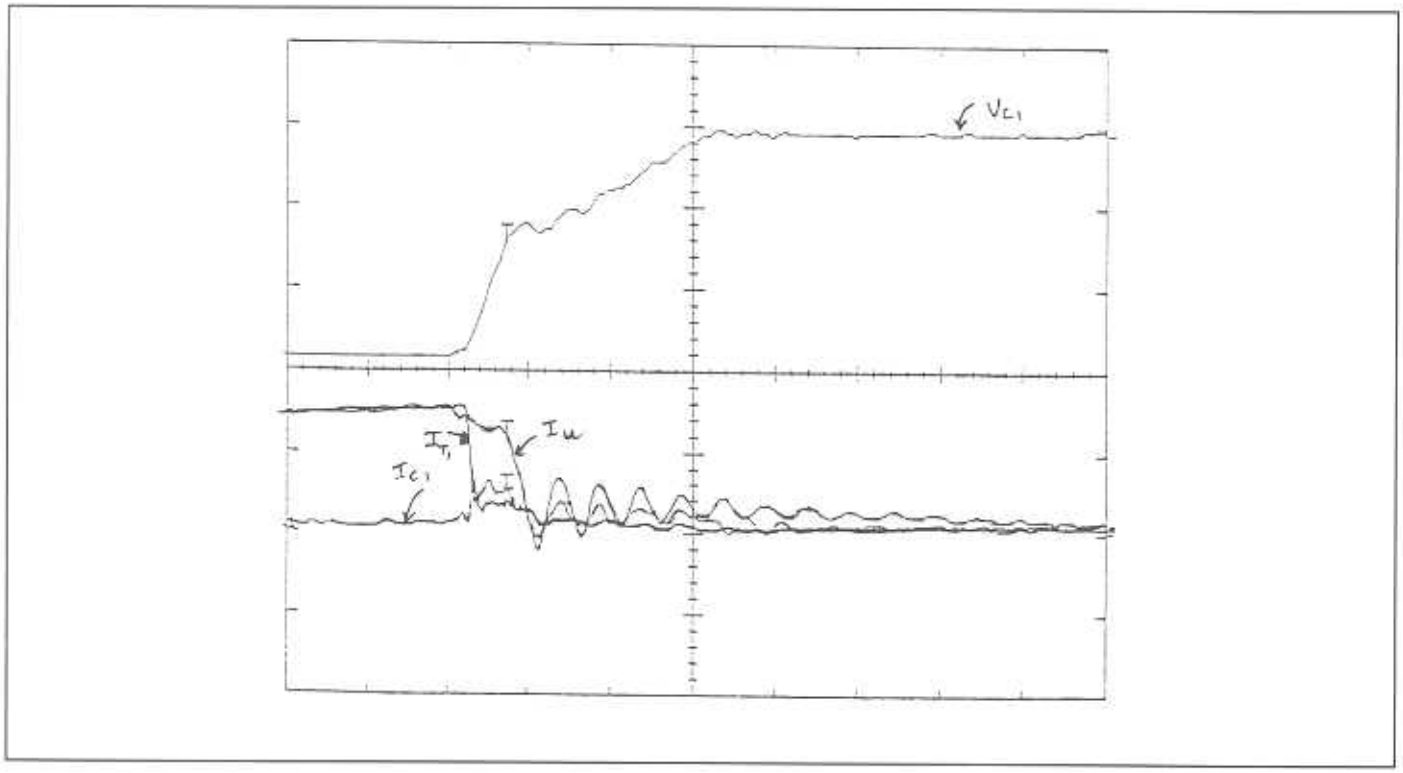

Figure 10. Voltage and current wave-forms during commutation with a transformer air gap of 0.3 mm.

The efficiency of the proposed DC/DC converter is experimentally investigated under different air-gaps and under different loading conditions. A summary of the most relevant experimental results is presented in table 2. The column efficiency, included in this table, indicates the maximum value observed for each air-gap and under the tested loading range.

Compromising among commutation time, switching spikes and efficiency, an empirical optimum is observed with an air-gap of about 0.9mm. The closed form theoretical and numerical investigation of the transformer air-gap effect on the proposed converter's performance (i.e. commutation time, switching spikes and efficiency), as well as the mathematical link between λ and the air-gap width are under investigation.

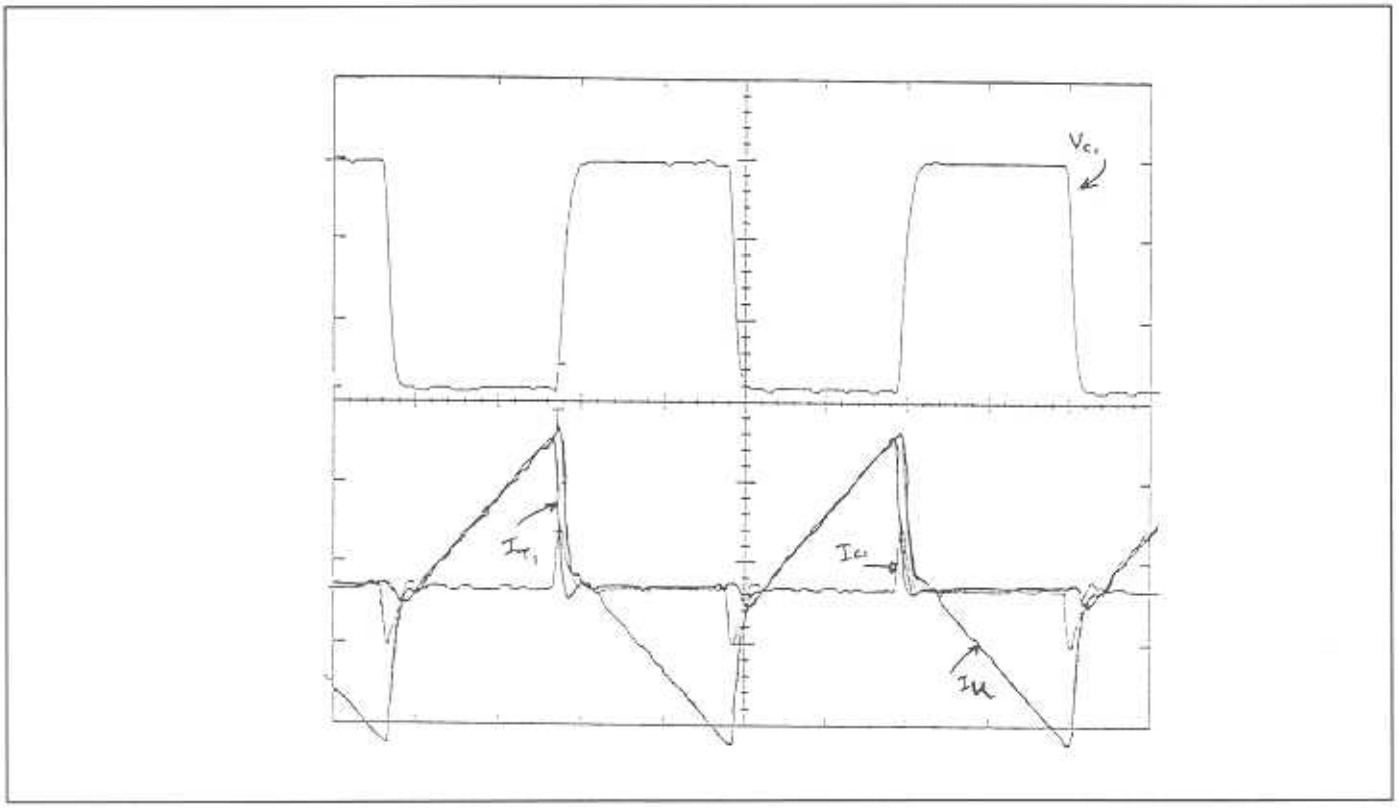

Figure 11. Voltage and current waveforms obtained with an air gap of 1.5 mm.

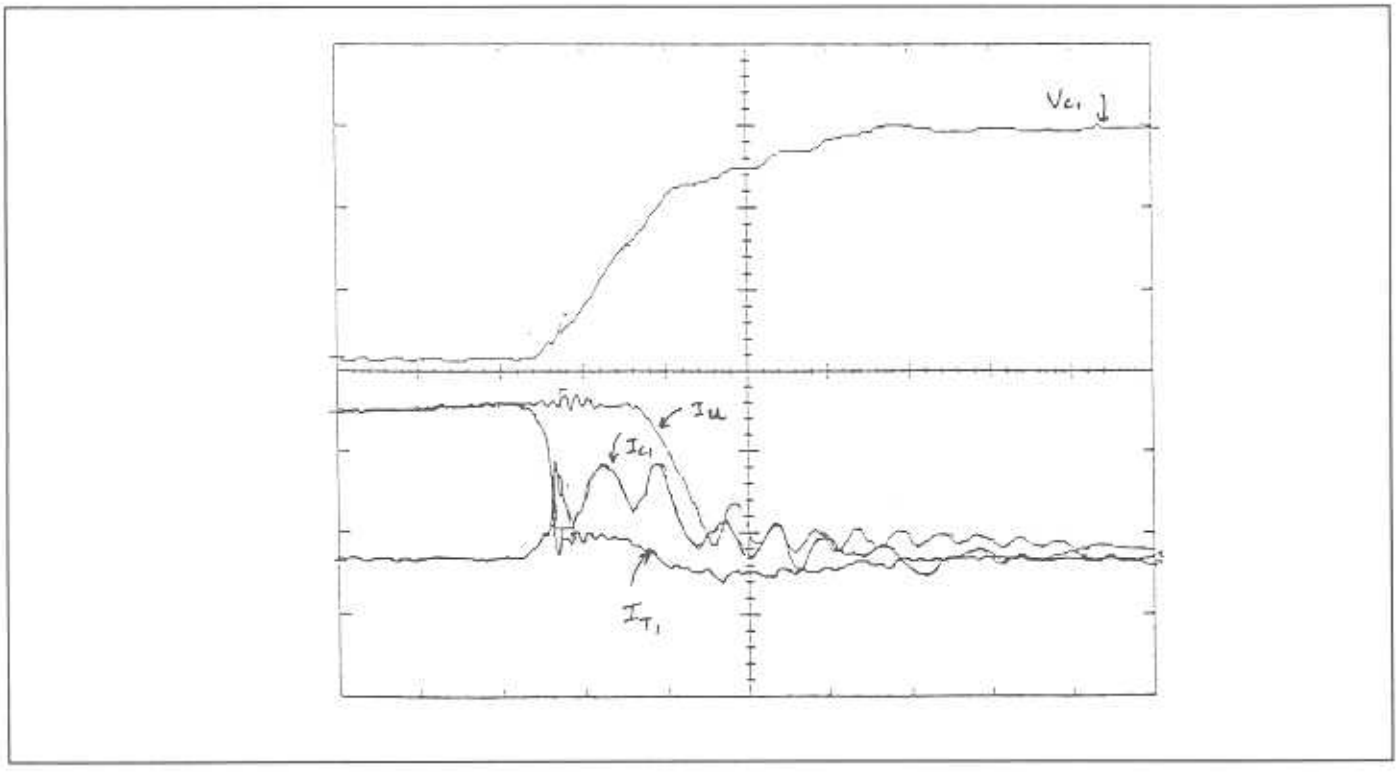

Figure 12. Voltage and current waveforms during commutation with a transformer air gap of 1.5 mm.

TABLE 2

Summary of salient experimental results of the proposed DC/DC converter.

Airgap (mm)	L_m (mH)	t_{d1} (μsec)	t_{d2} (μsec)	η (%)	Input voltage (V)	Input current (A)	Output voltage (V)	Output current (A)
0.3	1.54	0.5	1.5	92	300	1.25	278	1.2
0.6	0.95	0.4	1.4	95	300	1.75	289	1.72
0.9	0.80	0.3	1.3	95	300	2.5	287	2.48
1.5	0.47	0.6	1.7	90	300	3.5	724	3.45

Conclusion

The analysis and design of an indirect DC-DC converter are presented in this paper. IGBT power modules are used in the DC-AC conversion, and a variable air-gap transformer is employed in the resonant ac link. The proposed converter is built and tested in the laboratory. The obtained experimental results are in good agreement with theoretical and PSPICE simulated results.

References

AKHERRAZ, M. 1993. Analysis and Design of a DC to DC Resonant Converter for Railroad Applications, Proceedings of *IEEE-ISIE*, Budapest, June 1-3, 1993, pp. 771-776.

BHAT, A.K.S. 1991 "A Resonant Converter Suitable for 650 V Dc Bus," *IEEE-PE*, **6**, pp. 739-748.

BHAT, A. K. S. 1993. Analysis and Design of a Modified Series resonant Converter, *IEEE-PE*, **8**, pp.423-430.

BOSE, B. K. 1992 (edit.), *Modern Power Electronics*, New York, IEEE Press.

BOSE, B. K., 1992 "Recent Advances in Power Electronics," *IEEE-PE*, 7, pp. 2-16.

D. S. LO, et al, 1992. " A Compact Dc to Dc Power Converter for Distributed Power Processing," *IEEE-PE*, 7, pp. 714-724.

M. H. RASHID, 1993. *Power Electronics. Circuits, Devices and Applications*, Second Edition, Prentice Hall.

M. K. KAZIMIERCZUK, et al, 1992 " Frequency Domain Analysis of Series Resonant Converter for Continuous Conduction Mode," *IEEE-PE*, 7, pp. 270-279.

P. JAIN, et al, 1992. " Analysis and Design of a High Frequency High Power Series Resonant Inverter Using Asymmetrical Thyristors," *IEEE-PE*, 7, pp. 693-706.

R.L.STEIGERWALd, 1984. " High frequency resonant dc-dc converters,"*IEEE-IE*, **31**, pp. 181-191.

R.P SEVERNS, 1992, "Topologies for Three-Element Resonant Converters," *IEEE-PE*, 7, pp. 89-98.

S. MORRISON, 1992. "Analysis of a Hybrid Series Parallel Resonant Bridge Converter," *IEEE-PE*, 7, pp. 119-127.

T. NINOMIYA, et al, 1991. "A Unified Analysis of Resonant Converters," *IEEE-PE*, **6**, pp 260-270.

Received 9 March 1996
Accepted 24 September 1997